Pushing the limits of the CyberGrasp™ for haptic rendering

Manuel Aiple and André Schiele

Abstract— The CyberGrasp™ is a well known dataglove-exoskeleton device combination that allows to render haptic feedback to the human fingers. Its design, however, restricts its usability for teleoperation through a limited control bandwidth and position sensor resolution. Therefore the system is restricted to low achievable contact stiffness and feedback gain magnitudes in haptic rendering. Moreover, the system prohibits simple adaption of its controller implementation.

In this paper, the ExHand Box is presented, a newly designed back-end to widen the CyberGrasp™'s bandwidth restrictions and to open it up for fully customized controller implementations. The ExHand Box provides a new computer, interface electronics and motor controllers for the otherwise unmodified CyberGlove® and CyberGrasp™ hand systems. The loop frequency of the new system can be freely varied up to 2 kHz and custom controllers can be implemented through an automatic code generation interface.

System performance identification experiments are presented that demonstrate improved behavior in hard contact situations over a range of sampling periods. Maximum contact stiffnesses of up to 50kN/m in a stable condition are demonstrated, which is significantly higher than what could be achieved with the non-customized original system version.

Moreover, a bilateral control experiment is conducted to demonstrate the new system's usability for generic teleoperation research. In this experiment a raycasting algorithm is introduced for pre-contact detection in order to compensate for high delay and jitter communication links between master and slave as they appear in an Ethernet network. It is demonstrated that the contact stiffness can be maintained in the order of magnitude of the system performance identification with a demonstrated stiffness of 41kN/m in a stable condition.

I. INTRODUCTION

The CyberGrasp™, a product of CyberGlove Systems LLC, is a hand-grounded force-feedback device to provide haptic feedback to the fingers of the hand. It is designed to be used together with the separately available CyberGlove® dataglove that provides joint angle information of the hand and fingers. This combination of the two devices has been used in research in different domains, e.g. in haptic rehabilitation [2], in training of visually impaired [3] and in industrial training applications [4]. Within the Telerobotics & Haptics Laboratory at the European Space Agency (ESA), the CyberGrasp system has been used for studies on user performance depending on visual- and force-feedback quality during teleoperated grasping [1].

Fig. 1. The ExHand Box with CyberGrasp™ and CyberGlove® connected. The only external interface required is power through a laptop-like supply.

In order to extend the commercial form of the CyberGrasp™ for optimal usability in teleoperation research, following improvements are important:

- Increase the control bandwidth by at least a factor of ten.
- Add flexibility in controller prototyping.
- Reduce the amount of hardware (the commercial version requires a desktop-PC sized controller computer, the CyberGlove® electronics interface unit, the CyberGrasp™ motor box).

It is well known that time discretization, bandwidth limitations as well as position and other sensor quantization effects limit the maximum stable feedback gains that can be achieved with a given haptic device [5] [6]. Especially the sampling rate limitation of the CyberGrasp™ system at 90 Hz is a limiting factor for achievable high wall stiffnesses in rendering scenarios and for overall telerobotics implementations. While the position sensor quantization is adequate, with a 1000 pulse per revolution encoder, no gearing is implemented between the motor and the cable outputs of the CyberGrasp™. In total, this severely restricts the achievable contact stiffness of the system in haptic applications in virtual or real contact environments. At the same time, the mechanical implementation of the CyberGrasp™ incorporates cable transmissions, which can have positive effects on stabilizing an haptic system through small amounts of naturally occurring viscous and Coulomb friction (e.g. damping).

Therefore we initiated the new design of the back-end electrical and computing interface of the CyberGrasp™ system, which resulted in the development of the ExHand Box (Fig. 1).

The new ExHand Box was designed with following requirements:

- Achievable control loop frequency more than 1kHz.
- Controller programmable via MATLAB/Simulink.
- Small hardware configuration with one table-top box including all required subsystems.

It is the goal of this paper to present the design of the new ExHand Box system for teleoperation research. A system performance identification experiment will be carried out to quantify the achievable feedback characteristics of the new system. Experimentally achievable feedback loop frequencies and their maximum feedback stiffness/damping gains will be determined during stable and passive interaction with virtual walls. Furthermore, a practical example for its use in a bilateral control application with a dexterous robot hand simulation will be given.

II. EXHAND BOX SYSTEM OVERVIEW

In the process of redesigning the CyberGrasp™ all electronics were stripped off and replaced. The only components remaining of the original system are the dataglove and the exoskeleton with the motors (without motor drives).

Figure 2 shows an overview of the new system. All signals between the dataglove and the controller and between the controller and the exoskeleton are sampled at the step size of the model running on the controller which can be configured up to 2kHz. The current control loop of the new motor drives runs at 4kHz.

The controller is a PC with a 1.6GHz Intel Atom processor according to the PC/104 standard running the xPC Target real-time operating system.

The sensor information from the 22 sensors in the dataglove is amplified and filtered by 22 independent amplifier and filter chains. A Diamond MM-32X-AT Analog I/O board is used to sample the amplified sensor signal with a resolution of 0.3mV (22bit resolution over the amplified signal voltage range). Its multiplexed maximum sample rate is 250kHz.
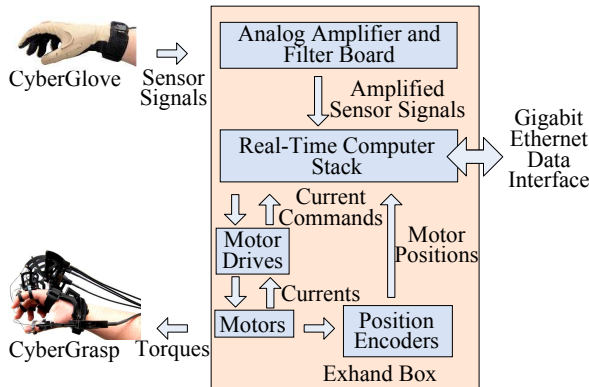
The motor position encoders are 1000 pulse per turn quadrature encoders and their signals are decoded using two Sensoray S526 boards. These also have four D/A channels and eight A/D channels, some of which are used to control the analog servo motor drives and to monitor the motor currents. The motor drives used are miniature Elmo Castanet with a maximum continuous current of 3.3A and a maximum peak current of 6.6A. Table I summarizes the relevant measured resolutions of the ExHand controller. The estimated quantization is conservative, since the peak-to-peak noise level of the actual signals has been used. The signals are stable (i.e. not flipping) to the specified number of bits.

The controller and the motors are powered with 24VDC. The data connection to the controller is implemented through Gigabit Ethernet.

The complete box with controller, motors, motor drives and analog electronics measures 250mm x 210mm x 155mm with a mass of 4kg and is entirely self sustained.

III. SYSTEM STEP RESPONSE IDENTIFICATION

A. Experimental Setup

In order to identify the step response characteristics of the system at different gain settings an experiment was carried out which consisted in letting a mass m fall from a given height h and make the system stop its fall (Fig. 3). This tests the response of the system for collision rendering at high speed. It is important to note here, that the force output of the system can not be measured directly through a sensor, therefore calibrated masses have been used to determine an exact force input step.

The mass used for this experiment was 500g and the free fall height 7cm.

The controller model used for this experiment is depicted in figure 4.

The model uses the motor encoder information to determine if the virtual contact condition applies or not. This is the case if the position reaches the collision threshold which corresponds to the free fall height h. In this case the force command $F_{contact}$ as calculated according to equation 1 applies.

Fig. 2. Overview of the ExHand Box system. The CyberGlove® sensor input is amplified and filtered by the ExHand Box and torques are provided to the CyberGrasp™ for haptic feedback. The system can communicate with a slave device via a Gigabit Ethernet link.
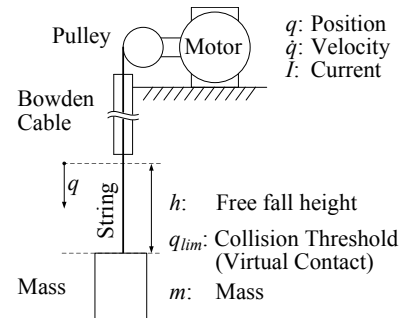
Fig. 3. Schematic of the experimental setup. The mass is dropped from a rest position and stopped by the controller when reaching the virtual contact. The virtual contact is defined by the motor position which corresponds to the free fall height.
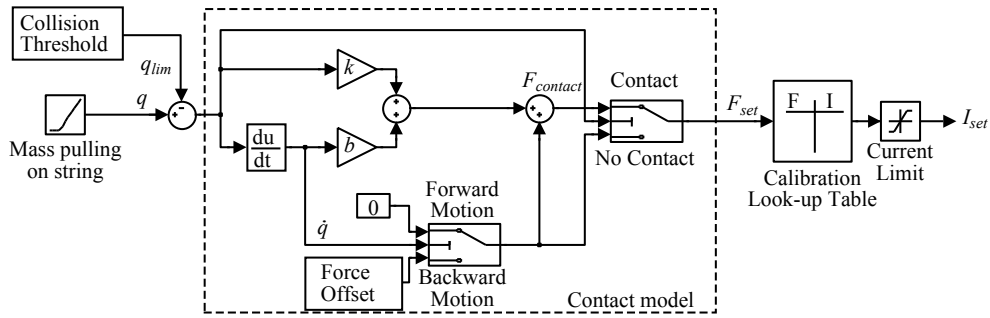
Fig. 4. Representation of the controller model used for the step response performance identification. q: motor position; $\dot{q}$: motor velocity; q_{lim}: virtual contact position; k: virtual spring constant; b: virtual damper constant; $F_{contact}$: calculated contact force; F_{set}: force command; I_{set}: current command;

TABLE I
SIGNAL RESOLUTIONS OF THE EXHAND CONTROLLER

Signal	Noise Level (Peak-to-Peak)	Resolution (Stable Bits)
Joint Angle	6.1mV	11
Motor Position	1 encoder step	9
Current	47.2mA	7

$$F_{contact} = b\dot{q} + kq + F_0 \tag{1}$$

With b being the damping factor (in Ns/m), k the spring constant (in N/m) and q the mass' position with respect to the collision threshold. F_0 is the pullback force which is null if the string is pulled out (i.e. if $\dot{q} >= 0$) and large enough to overcome the friction in the Bowden cable and pull the string back on the pulley if the string is released (i.e. if $\dot{q} < 0$). This can be tuned with a "Force Offset" parameter.

If the contact condition does not apply, the force command F equals F_0. In the contact situation the model corresponds to a PD-Controller with the proportional gain equal to k and the derivative gain equal to b.

B. Experimental Method

Before any experiments, the system was calibrated to determine the conversion table from desired force to the current command signal and the conversion table from motor current monitoring signal to force on the string in the SI system.

The experiment was carried out for loop frequencies of 90Hz (corresponding to the original system), 100Hz, 200Hz, 500Hz, 1000Hz and 2000Hz. Every test run consisted of ten falls. After every run the parameters k and b were increased until the system became unstable for the given frequency, then the loop frequency was increased. The system was considered unstable when it oscillated continuously after the virtual collision instead of coming to rest at an end position.

During the experiments, the following data was logged on the controller with the loop frequency at which the model was running:

- experiment time t (s)
- position q (m)

- speed $\dot{q}$ (m/s)
- force command F_{des} (N)
- current command I_{des} (A)
- collision condition applying c (true | false)
- force calculated from the motor current monitoring signal F_{mon} (N)

The *collision condition applying* signal was used to dissect the log data of the ten falls into ten separate contact situations.

On the basis of the monitored force and position data of the contact situations the stiffness was calculated. Therefore, the position and force data pairs of all contact situations were taken together. Then the data pairs with a force value out of the range of 0.8N to 4.5N were rejected in order to take into account only points on the slope and remove the data points corresponding to the time before letting the mass fall and after it was stopped by the motor.

The remaining pairs were sorted by increasing force. Then a ten values unweighted moving average was calculated over the position values in order to reduce the effect of outliers on the following linear regression.

Finally a linear regression was calculated over these new position and force data pairs to get the stiffness as ratio of force over position.

C. Results & Discussion

Figure 5 shows the experimental stability results of the system with different loop frequencies in the k-b-space. By increasing the loop frequency to 2000Hz, the parameters k and b can be nearly 20 times higher than with the original frequency of 90Hz.

Table II shows how this affects the achievable stiffness. When comparing table II and figure 5, attention should be paid to the fact that the experiment with the highest stable parameters for the respective loop frequency is not necessarily the one that gave the maximum stiffness as calculated from the force over position curve.

The maximum achieved stiffness of the virtual contact is 36 times higher with a loop frequency of 2000Hz than with 90Hz (Fig. 6). This means that contacts can be rendered with higher crispness with the ExHand Box controller than with the original CyberGrasp[TM] setup.
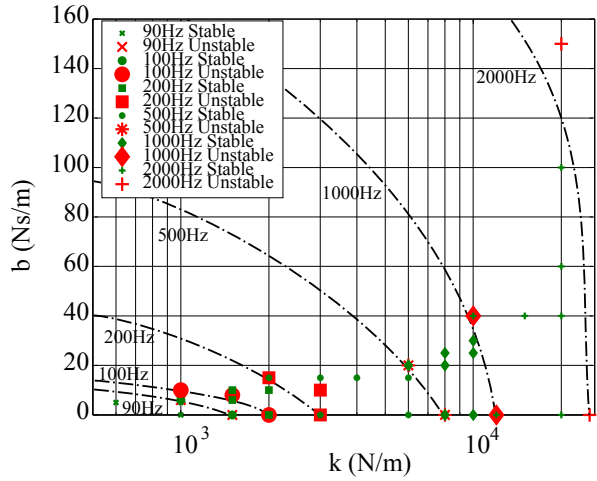
Fig. 5. Stability of the system in the *k-b*-space for different loop frequencies. The dot-dashed lines are very roughly estimated stability borders at the respective loop frequency for indication only.

TABLE II

MAXIMUM ACHIEVED STIFFNESS FOR DIFFERENT LOOP FREQUENCIES

Frequency (Hz)	k (N/m)	b (Ns/m)	Stiffness (N/m)
90	1500	0	1374
100	2000	0	1506
200	2000	15	7203
500	6000	20	11977
1000	10000	40	18936
2000	20000	60	50004

IV. BILATERAL CONTROL EXPERIMENT

A. Experimental Setup

A simple scenario of collision with virtual objects was chosen to test the haptic rendering quality of virtual contacts with the ExHand Box. In this scenario a person wearing the dataglove and exoskeleton should be able to control a virtual hand and feel the contact with virtual objects. For this purpose a World Simulator (virtual slave robot hand) program was written, running on an independent computer connected to the ExHand Box (master controller) via a Gigabit Ethernet connection (Fig. 7).

B. Experimental Method

The world simulator is responsible for the visualization of the virtual hand and the virtual world (Fig. 8). Depending on the complexity of the world model it renders the scene at a frame rate of 100-400fps. This frame rate corresponds to the frequency at which it receives from and sends data to the ExHand controller.

It receives the joint angles for the virtual robot hand from the master controller which feed a virtual model of the Hit Hand II from German Aerospace Center (DLR). The mapping of CyberGlove®sensor signals to Hit Hand II joint angle values is done on the ExHand controller using the mapping model developed for [1].
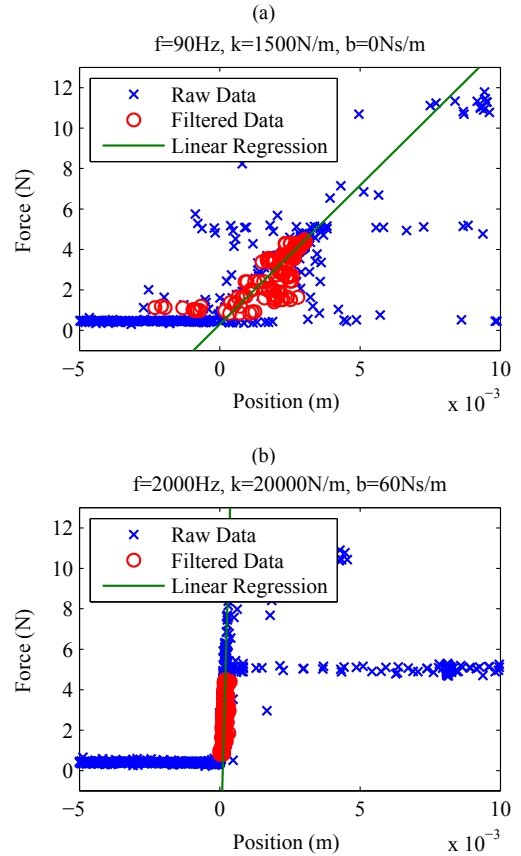
Fig. 6. Force over Position plot from the performance identification, *(a)* for $f = 90$Hz, $k = 1500$N/m, $b = 0$Ns/m. The calculated stiffness is 1374N/m. *(b)* for $f = 2000$Hz, $k = 20000$N/m, $b = 60$Ns/m. The calculated stiffness is 50004N/m. Blue crosses: raw data, red circles: filtered data for regression, green line: linear fitting to the filtered data points.
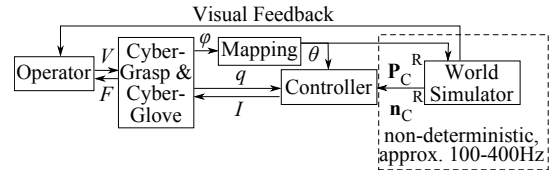
Fig. 7. Principle of the bilateral control application. V: finger velocity; F: feedback forces; φ: glove joint angles; θ: robot joint angles; q: motor positions; I: motor currents; $\mathbf{P}_C^R$: collision plane point coordinates in the robot hand frame; $\mathbf{n}_C^R$: collision plane normal vector;
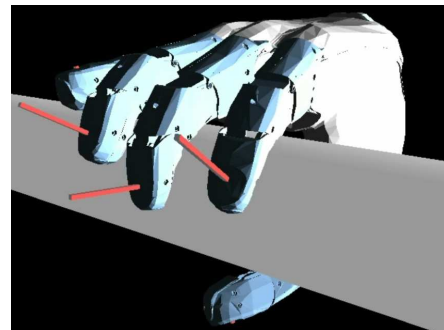
Fig. 8. The visualization of the world simulator, the red bars show the contact forces.

Special care was taken to not negatively influence the performance of haptic rendering by a non-deterministic bilateral link with variable delay and jitter. This was achieved by keeping the collision detection completely on the controller side and by introducing a pre-contact detection algorithm to change the collision parameters on-line between master and slave.

Figure 9 shows a schematic view of this algorithm. The World Simulator receives the robot finger joint angles θ from the ExHand controller and calculates the position of the point P_F in the virtual world, with P_F representing the point in the middle of the finger tip. It then does a raycast from P_F in the direction $\mathbf{r}$. If the ray hits a virtual collision object O, the coordinates of the collision point P_C in the virtual world and the normal vector $\mathbf{n}_C$ of the surface of O at the point P_C are determined. P_C and $\mathbf{n}_C$ define the collision plane H. The world simulator translates the coordinates of P_C and $\mathbf{n}_C$ into the robot hand frame, notated $\mathbf{P}_C^R$ and $\mathbf{n}_C^R$ respectively. It then sends $\mathbf{P}_C^R$ and $\mathbf{n}_C^R$ to the ExHand controller.

The ExHand controller also uses θ to calculate the robot finger tip position $\mathbf{P}_F^R$ in the robot hand frame {R}. It then calculates the distance d, which is the point-plane-distance between P_F and H minus the radius of the fingerpad t. d is defined according to equation 2, such that it is negative before the contact and positive in the contact.

$$d = (\mathbf{P}_C^R - \mathbf{P}_F^R) \cdot \mathbf{n}_C^R - t \qquad (2)$$

Figure 10 depicts the model running on the ExHand controller.

The distance d is used to do a reverse mapping from the robot task space to the CyberGrasp™ joint space. It modifies $q_{lim}(t)$, the position of the virtual contact q_{lim} at a time t according to the rule in equation 3.

$$q_{lim}(t) = \begin{cases} q_{lim}(t-dt) & \text{if } d \geq d_{lim} \\ d & \text{otherwise} \end{cases} \qquad (3)$$

Where d_{lim} is a negative constant defining the threshold where the controller should switch into contact mode and dt is the simulation time step. Thus $q_{lim}(t-dt)$ refers to the value of q_{lim} in the previous iteration of the simulation loop.

The effect of this rule is that once the robot fingertip is in a critical distance to the virtual collision object, q_{lim} is frozen and the remaining way to the contact and the contact rendering itself is independent of the world simulator. This effectively decouples the high frequency contact rendering on the ExHand controller from the constraints of the non-deterministic bilateral link with the world simulator.

As can be seen, the contact model itself is the same as in the step response performance identification controller model.

Different system parameters were experimented with in the bilateral control configuration, demonstrating higher perceived crispness with higher values of k and b as expected.

In the following, the experiment with the system parameters set to the values identified in the system performance
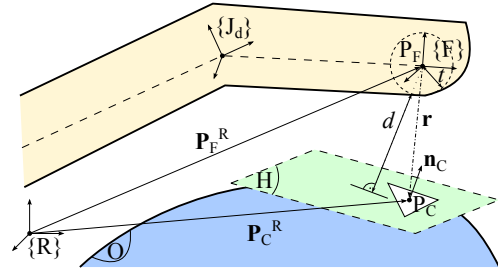
Fig. 9. Pre-contact detection principle. {R}: robot hand frame; {F}: finger tip frame; {J_d}: distal joint frame of the robot hand; O: collision object; P_F: finger tip center point, origin of raycast; $\mathbf{r}$: direction of raycast; P_C: collision point where the ray hits O; $\mathbf{n}_C$: normal vector of O at P_C; H: collision plane defined by P_C and $\mathbf{n}_C$; d: distance between P_F and H; $\mathbf{P}_F^R$: coordinates of P_F in {R}; $\mathbf{P}_C^R$: coordinates of P_C in {R}; t: radius of the fingerpad;

identification as the ones with the highest stiffness will be discussed, i.e. $f = 2000\text{Hz}$, $k = 20000\text{N/m}$, $b = 60\text{Ns/m}$.

The test subject was asked to enter into contact situation several times at different speeds: as slowly as possible, at what seemed to be a natural speed, and as fast as possible.

The following signals were logged:

- experiment time t (s)
- position measured by the motor encoders q (m)
- speed measured by the motor encoders $\dot{q}$ (m/s)
- force command F_{des} (N)
- current command I_{des} (A)
- collision condition applying c (true | false)
- force calculated from the motor current monitoring signal F_{mon} (N)
- distance to collision plane calculated from the dataglove input through the hand model and the collision plane information d (m)
- collision threshold q_{lim} (m)

C. Results & Discussion

Figure 11 shows a plot from a typical contact situation at medium speed (0.87m/s when entering into the virtual contact). The system response settles approximately 25ms after the first contact into a stable equilibrum. For the test subject this transient was not noticeable, but mechanical damping by the pulling string might have effects in this as well which were not investigated further.

Figure 12 shows the force over position plot from a run with the bilateral control experiment. It confirms the order of magnitude of the stiffness values (the calculated stiffness for this run was 41250N/m) from the step response performance identification also in bilateral control applications, thus proving the positive effects of the pre-contact detection mechanism.

V. CONCLUSION

It has been shown that using CyberGlove®and CyberGrasp™with the new ExHand Box improves their performance significantly, with an increase of the stiffness of up to 50kN/m, thus achieving a stiffness 36 times higher than before and enabling crisper rendering of hard contacts.
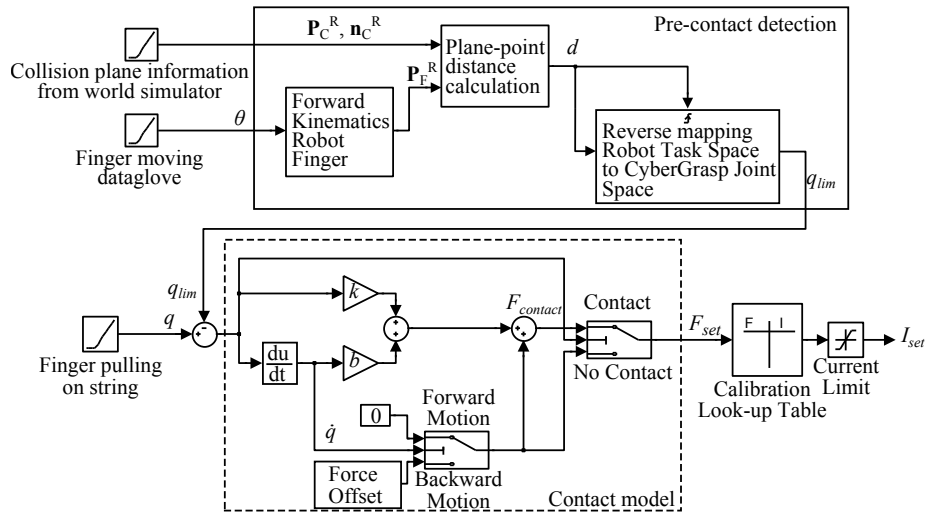
Fig. 10. Representation of the controller model used for the bilateral control experiment. q: motor position; $\dot{q}$: motor velocity; θ: robot joint angles; $\mathbf{P}_F^R$: robot fingertip coordinates in robot hand frame; $\mathbf{P}_C^R$: virtual collision plane point vector in robot hand frame; $\mathbf{n}_C^R$: virtual collision plane normal vector in robot hand frame; d: distance between robot fingertip and virtual collision plane; q_{lim}: virtual contact position; k: virtual spring constant; b: virtual damper constant; $F_{contact}$: calculated contact force; F_{set}: force command; I_{set}: current command;
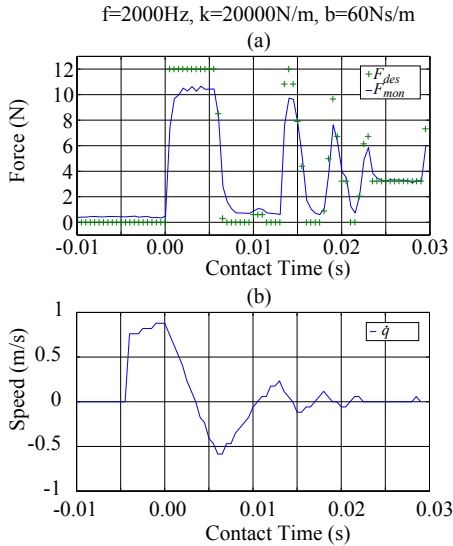
Fig. 11. Time plot of a typical contact situation at 0.87m/s contact speed for $f = 2000\text{Hz}$, $k = 20000\text{N/m}$, $b = 60\text{Ns/m}$. (a) green crosses: force command F_{des}, blue line: force calculated from the motor current monitoring signal F_{mon}. The black vertical line shows the beginning of the contact. (b) speed $\dot{q}$.

Fig. 12. Force over Position plot from the bilateral control application for $f = 2000\text{Hz}$, $k = 20000\text{N/m}$, $b = 60\text{Ns/m}$. The calculated stiffness is 41250N/m. Blue crosses: raw data, red circles: filtered data for regression, green line: linear fitting to the filtered data points.

The new controller of the ExHand Box can be easily customized in MATLAB/Simulink with auto-code generation, achieving loop frequencies of up to 2kHz. Therefore, it provides a platform to test different controller models.

A raycasting algorithm has been implemented successfully in a bilateral control experiment for pre-contact detection to achieve similarly high performance of 41kN/m stiffness in a delay and jitter biased scenario where master and slave device communicate via a typical non-dedicated Ethernet network.

ACKNOWLEDGMENT

REFERENCES

[1] N. Y. Lii, Zhaopeng Chen, B. Pleintinger, C. H. Borst, G. Hirzinger, and A. Schiele, "Toward Understanding the Effects of Visual- and Force-Feedback on Robotic Hand Grasping Performance for Space Teleoperation," in Proc. 2010 IEEE/RSJ International Conference on Intelligent Robots and Systems, Taipei, 2010 pp. 3745-3752.

[2] J. Zhou and F. Malric, S. Shirmohammadi, "Practical Calibration for Upper Extremety Patients in Haptic Rehabilitation," Intern. Workshop on Medical Measurements and Applications, Cetraro, 2009, pp. 73-78.

[3] D. Tzovaras, G. Nikolakis, G. Fergadis, S. Malasiotis, and M. Stavrakis, "Design and Implementation of Haptic Virtual Environments for the Training of the Visually Impaired," IEEE Trans. Neural Systems and Rehabilitation Eng., vol. 12, no. 2, pp. 266-278, Jun. 2004.

[4] M. Hosseini, F. Malric, N. D. Georganas, "A Haptic Virtual Environment for Industrial Training," IEEE Intern. Workshop Haptic Virtual Environments and Their Applications, 2002, pp. 25-30.

[5] N. Diolaiti, G. Niemeyer, F. Barbagli, J. Kenneth Salisbury, "Stability of Haptic Rendering: Discretization, Quantization, TimeDelay, and Coulomb Effects," IEEE Trans. on Robotics, Vol. 22, No. 2, April 2006, pp. 256 - 268.

[6] J.J. Abbott and A.M. Okamura, "Effects of position quantization and sampling rate on virtual-wall passivity," IEEE Trans. on Robotics, Vol. 21, No. 5, March 2005, pp. 952 - 964